molecules

MDPI

Review

The Role of Sub- and Supercritical CO_2 as "Processing Solvent" for the Recycling and Sample Preparation of Lithium Ion Battery Electrolytes

Sascha Nowak [1,*] and Martin Winter [1,2]

[1] University of Muenster, MEET Battery Research Center, Corrensstraße 46, 48149 Münster, Germany; martin.winter@uni-muenster.de
[2] Helmholtz Institute Münster, IEK-12, Forschungszentrum Jülich, Corrensstraße 46, 48149 Münster, Germany
* Correspondence: sascha.nowak@uni-muenster.de; Tel.: +49-251-833-6735

Academic Editor: Yu Yang
Received: 30 January 2017; Accepted: 27 February 2017; Published: 6 March 2017

Abstract: Quantitative electrolyte extraction from lithium ion batteries (LIB) is of great interest for recycling processes. Following the generally valid EU legal guidelines for the recycling of batteries, 50 wt % of a LIB cell has to be recovered, which cannot be achieved without the electrolyte; hence, the electrolyte represents a target component for the recycling of LIBs. Additionally, fluoride or fluorinated compounds, as inevitably present in LIB electrolytes, can hamper or even damage recycling processes in industry and have to be removed from the solid LIB parts, as well. Finally, extraction is a necessary tool for LIB electrolyte aging analysis as well as for post-mortem investigations in general, because a qualitative overview can already be achieved after a few minutes of extraction for well-aged, apparently "dry" LIB cells, where the electrolyte is deeply penetrated or even gellified in the solid battery materials.

Keywords: supercritical CO_2; subcritical CO_2; liquid CO_2; lithium ion battery electrolytes; lithium ion battery; recycling; sample preparation; aging; post-mortem

1. Introduction

Due to unrivalled high energy densities and high specific energies, lithium ion batteries (LIBs) are used in everyday modern portable consumer electronics, such as tablets, smartphones and laptops. Furthermore, they are considered the most promising battery technology for pure electric and hybrid electric vehicles (xEVs) [1–3] and, due to high energy efficiencies, also for stationary energy storage applications [4]. This widespread application for private and industrial purposes will inevitably raise a demand for reutilization and recycling of the lithium ion battery components. Due to the high prices of Ni and Co, which are deployed in the form of oxides in the LIB cathode, and of Cu used as current collector at the anode [5], recycling is also of economic interest. Recycling processes for the metals in the cathode already exist. The recycling value of these metals would, however, be increased if direct recovery as ready to use battery raw constituents were possible. However, the high purity requirements of the battery material manufacturers diminish this approach. In addition, the recycling of LIBs or its single constituents is encouraged by legislation. Lithium, for example, has no actual substitute and due to its growing application, the demands might exceed the global production by the 2020s [6,7]. Therefore, Li recycling needs to be established. For the EU, limited occurrences were reported, e.g., in Portugal [8,9] or the Czech Republic [10]. Thus, the European Parliament and Council of the European Union issued several directives such as the Waste of Electrical and Electronic Equipment (WEEE) 2012/19/EU and the End of Life Vehicles (ELV) 2000/53/EC, which deal with the recycling of batteries from electronic products and electric vehicles. Beginning in 2016, at least 45 wt % of

electrical and electronic equipment needs to be collected by the EU members. The reuse and recovery rate for end of life vehicles is set to at least 85% regarding both the weight per vehicle and the calendar year. Furthermore, the Battery Directive 2006/66/EC was instituted as the most advanced battery recycling legislation worldwide. Each EU member state has to meet a collection rate of 45% and at least a recycling efficiency of 50 wt % for non-lead-acid and non-nickel-cadmium batteries [11–13].

With regard to upcoming pilot processes and plants, the LIB aging has to be taken into account. New or only lightly used LIBs from electric vehicles are not the focus of recycling strategies. Foremost, damaged batteries or batteries that have achieved the end of life (EOL), i.e., strongly aged batteries, are in the focus of recycling. Aging is one of the main performance deteriorations of LIBs as aging leads to capacity loss, resistance increase, power and energy loss and therefore to a reduced lifetime [14,15]. Aging may also be responsible for safety changes of batteries [16]. However, there is no "universal aging mechanism"; in fact, numerous aging mechanisms occur and they can affect each other. Reports in the literature usually focused on the individual parts of the LIB cell such as the reactions between the electrolyte and the anode, solid electrolyte interphase (SEI) growth, the decomposition of cathode and anode, or lithium metal deposition on the anode [17–29] or on the interaction between the different materials [30]. Additionally, the operating conditions have a great influence of the degradation behavior [31–33]. However, the decomposition of the electrolyte is challenging to investigate due to its complex composition. Because of the sensitivity towards water and thermal influence, the literature reveals numerous reports about aging products and mechanisms. The variety of decomposition products includes HF [34–40], inorganic and organic (fluoro)phosphates (OPs) [41–48], CO_2 [49,50], dicarboxylates and oligocarbonate based products [51–53], diols [54] and alkyl fluorides [36,45,50]. Furthermore, the applied analysis methods and corresponding reaction mechanisms have been intensively discussed in literature and new reports are constantly added [55,56].

Especially, the fluorinated decomposition compounds and, in particular HF, are in special focus with regard to pilot processes and plants, since, due their chemically aggressive nature and their toxicity, they can seriously hamper or damage the industrial recycling approaches. Therefore, these compounds need to be removed before the recycling process. However, aged LIBs, where the liquid electrolyte is partially decomposed into solid and gaseous products, often appear as "dry". During operation, the electrolyte immobilizes into the deeper layers of the electrode and into the solid electrolyte decomposition products and can therefore not easily be recovered either for simple removal or subsequent analysis.

Sub- and supercritical CO_2 are attractive extraction tools for overcoming both challenges. While it is still a young research field, the usage of CO_2 as a recycling or sample preparation tool for the recovery and analysis of materials is repeatedly found in the literature in the last years.

2. Lithium Ion Batteries Electrolytes

Lithium ion batteries consist of a carbon/graphite based anode, a lithium transition metal oxide cathode and an electrolyte soaked polyolefin-based separator [57,58]. The electrolyte inside a lithium ion battery has to fulfill several requirements: wide electrochemical stability window, high ionic conductivity and redox stability are some of the desired requirements [59]. Additionally, the chemical and electrochemical compatibility with the other cell constituents should be ensured; furthermore, the electrolyte should be non-toxic, safe, environmentally friendly and cost efficient [60,61]. In order to meet these requirements, the electrolyte system typically consists of a conducting salt (1 M), dissolved in a mixture of different linear carbonates, e.g., dimethyl carbonate (DMC), ethyl methyl carbonate (EMC) or dimethyl carbonate (DEC), and a cyclic carbonate such as propylene carbonate (PC) or ethylene carbonate (EC) [62–64] (Figure 1). The most commercially applied conducting is lithium hexafluorophosphate ($LiPF_6$) (Figure 1) while alternatives such as lithium tetraborate ($LIBF_4$), lithium bis-(oxalato)borate (LiBOB) or ionic liquids (ILs) are possible [62,65–70]. Electrolyte additives are used up to 5%, either by weight or by volume [71]. Due to the application of additives, the electrolyte properties can be influenced: improvement of the flammability, enabling overcharge protection [71–73] or the SEI formation [25,74–78]. The SEI is formed during the first charge/discharge

(formation cycles) of the LIB cell and is essential for safety and performance due to its protection of the electrolyte from further reductive decomposition at the anode surface [79–81].

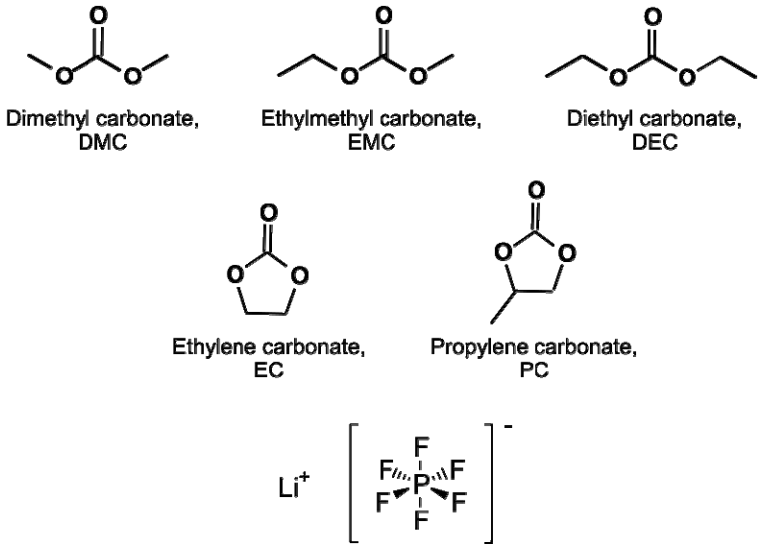

Figure 1. Structures of six of the most important linear and cyclic organic carbonates and the conducting salt lithium hexafluorophosphate for the electrolyte system in lithium ion batteries [60,61].

3. Aging of Lithium Ion Battery Electrolytes

For a better customer acceptance of LIBs, their capacity loss and therefore the reduction of their operating lifetime has to be minimized. The lifetime is limited by several aging mechanisms inside the cell and its components [14,15,30,82,83]. As stated in Section 2, the electrolyte is a mixture since it has to meet several requirements. Unfortunately, the salt lithium hexafluorophosphate is neither chemically nor thermally stable. A thermal equilibrium between $LiPF_6$ and LiF/PF_5 (Equation (1)) exists and PF_5 as a strong Lewis acid then further reacts with traces of water (present due to the high hygroscopicity of PF_6) to POF_3 (Equation (2)). With additional water, POF_3 is hydrolyzed to difluorophosphoric acid (Equation (3)), monofluorophosphoric acid (Equation (4)) and finally to phosphoric acid (Equation (5)) [35,84–88].

$$LiPF_6 \leftrightarrows LiF + PF_5 \quad (1)$$

$$PF_5 + H_2O \leftrightarrows 2HF + POF_3 \quad (2)$$

$$POF_3 + H_2O \leftrightarrows HF + HPO_2F_2 \quad (3)$$

$$HPO_2F_2 + H_2O \leftrightarrows HF + H_2PO_3F \quad (4)$$

$$H_2PO_3F + H_2O \leftrightarrows HF + H_3PO_4 \quad (5)$$

PF_5 can also initiate the transesterification of EMC to DMC and DEC (Figure 2a) [89]. Furthermore, the described hydrolysis products can react with the organic carbonate solvent to foster numerous organophosphate-based and organic fluorophosphate-based aging products (Figure 2c,d) [43]. Oligomeric carbonate-based decomposition products are formed by the electrochemically induced ring opening of EC and reaction with the linear carbonates (Figure 2b) [84,90,91]. The exact formation mechanism of the oligomeric carbonate-based compounds is still under discussion.

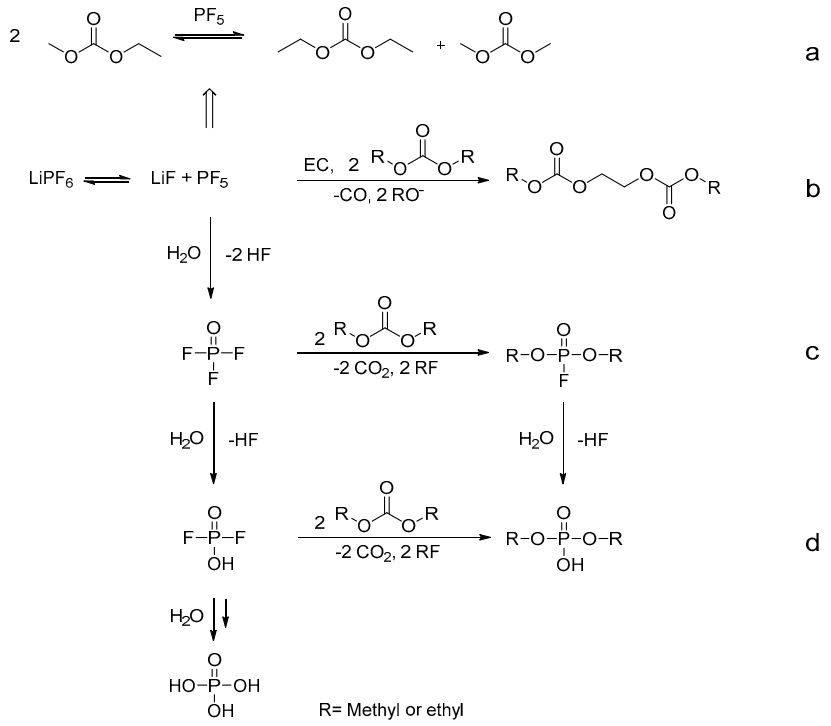

Figure 2. General decomposition pathways for the formation of: transesterifications products (**a**); oligocarbonate-based products (**b**); organophosphate-based products (**c**); organic fluorophosphate-based products; and hydrolysis products (**d**) [43,84–91].

The formed organic fluorophosphates have a high potential toxicity, and toxicological data are available for dimethyl fluorophosphate (DMFP) and diethyl fluorophosphate (DEFP) (Table 1). The LD_{50} value represents the amount of a solid or liquid material that it takes to kill 50% of the test animals in one experiment. The LC_{50} is the corresponding value for vapors, gases or dusts [92–100].

Table 1. Toxicity data for dimethyl fluorophosphate (DMFP) and diethyl fluorophosphate (DEFP) compared to the nerve agent sarin (mus = mouse; ivn = intravenous, skn = skin; ihl = inhalation; n/a = not available).

Compound	ivn-mus (LD_{50})	skn-mus (LD_{50})	ihl-mus (LC_{50})
Sarin	0.109 mg/kg	1.08 mg/kg	5 mg/m^3/30 min
DMFP	0.45 mg/kg	36 mg/kg	290 mg/m^3/10 min
DEFP	n/a	35 mg/kg	100 mg/m^3/10 min

The World Health Organization has five categories for hazardous substances with classified toxicity. Despite the lowered toxicity compared to sarin, according to toxicity data and classification, both DMFP and DEFP are classified in category 1, which is the most dangerous (fatal by swallowing <5 mg) and fatal by contact with the skin <40 mg/kg) [101]. Therefore, due to the P–F bond in many electrolyte decomposition products, they are considered hazardous as well. As an example, the neurotoxin diisopropyl fluorophosphate is known for its high toxicity as a consequence of the reaction with the enzyme acetylcholinesterase (AChE). The regular function of AChE is to hydrolyze acetylcholine, an essential neurotransmitter for the peripheral nervous system (PNS), which consists of the nerves and ganglia outside of the brain and spinal cord. The PNS is responsible for the connection of the central nervous system with limbs (skeletal muscle movement) and organs. By reaction between the organophosphate and AChE, a covalent bond is formed and the enzyme is stopped from regular functioning. This leads to an accumulation of unhydrolyzed acetylcholine and the symptoms of the intoxications are convulsions, suffocation and myosis, which ultimately can lead to death [102,103].

Besides the dangers regarding working safety when handling spent lithium ion batteries or shredded recycling waste, the fluorinated compounds and hydrofluoric acid can interfere or damage industrial scaled recycling processes and therefore have to be removed before the recycling process by extraction [104]. For post-mortem analysis and aging analysis of LIB electrolytes, extraction is inevitable, as well. While the electrolyte is introduced as a liquid during cell assembly, it penetrates and immobilizes in the electrodes during electrochemical operation (Figure 3). Thus, an opened LIB appears in most of the cases as "dry" after electrochemical operation.

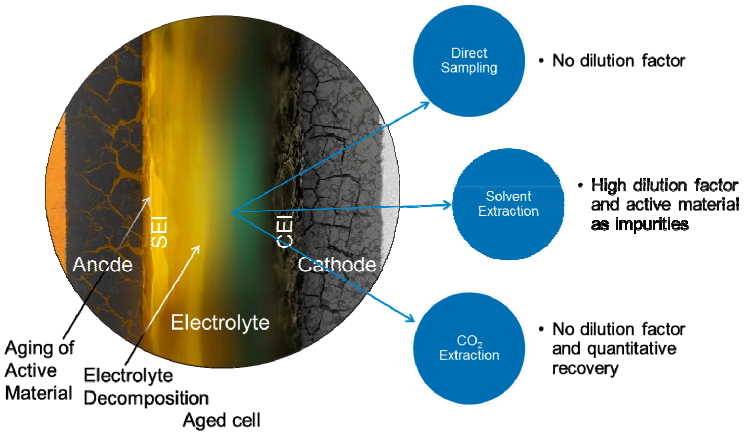

Figure 3. Schematic sketch of an aged lithium ion battery (LIB) and strategies for electrolyte recovery. CEI: cathode electrolyte interphase; SEI: solid electrolyte interphase.

Direct sampling of the electrolyte from a LIB, whenever possible, is the method of choice. However, it is seldom applicable. The extraction with an appropriate solvent can yield quantitative results but significant amounts of the electrode material are extracted as well and will be present as impurities. The extraction with sub- and supercritical CO_2 in comparison can yield quantitative results without a dilution factor.

4. Recycling of Lithium Ion Batteries Electrolytes

Lab-scale and commercial LIB recycling processes are focused on the recovery of the heavy metals (Ni, Co and Mn) and lithium itself from the cathode active material or on the current collectors, which consist of copper and aluminum [105–107]. The electrolyte is not recovered but simply combusted or disposed during the process or the handling of the electrolytes is not mentioned at all in the literature [108–110]. However, due to the directive 2006/66/EC from the European Parliament and the Council >50 wt % of LIB cell materials have to be recycled. The weight fraction of an electrolyte in a LIB cell is around 10–15 wt %, depending on the cell chemistry and geometry. The first approach for electrolyte recovery was the extraction with an appropriate regular solvent [108]. Nevertheless, general recycling procedures always referenced to the already published articles and procedures for electrolyte recycling [111–114]. Sloop et al. were the first to propose the application of supercritical carbon dioxide as an extraction medium for LIB electrolytes [115]. However, the given information about extraction conditions and the resulting extraction behavior is limited. In addition, the supercritical extraction procedure was not reported to be applied in a real recycling process, and not even on the lab-scale. However, compared to solvent extractions, the recycling efficiency with regard to the used amount of kg/CO_2 per kg/shredded material is in the same region for the reported methods.

Since spent LIBs are primarily from portable consumer applications and therefore only possess a limited amount of recyclable materials, the established pyro-hydrometallurgical recycling strategy by Umicore AG & Co. KG (Brussels, Belgium) is currently the most economic process [116]. Nickel metal hydride (Ni-MH) batteries and LIBs are delivered to a furnace and molten at temperatures of up to 1450 °C. With the help of co-added slag formers, Ni, Co and Cu form an alloy, while Li, Fe, Mn

and Fe accumulate inside the slag and are disposed. The organic cell components including the electrolyte are incinerated. In the following hydro-metallurgical step, the alloy fraction is separated and refined for re-utilization [116].

With the growing market for xEVs, the amount of spent LIBs will drastically increase. Considering several hundred kilograms of LIB cell material per car and taking into account that similar cell chemistries are used by the manufacturers, a continuous material flow is created. Therefore, a more holistic recycling process can be applied (Figure 4), including the recovery of the electrolyte [117]. This mechanical-hydrometallurgical process aims to meet the demands of the EU directive and therefore the utilization of most cell materials from a LIB. The deep discharged (by external resistance or power) battery packs are dismantled to the individual cell level and shredded in an inert atmosphere [108,114,118]. The electrolyte evaporated during this first step is collected by condensation. The electrolyte remaining in the shredded material is subject to three possible recovery methods: (i) a thermal drying step with the disadvantage of losing the conducting salt, which is the most costly component of the electrolyte; (ii) application of supercritical CO_2 in a static setup; and (iii) supercritical CO_2 in a flow-through setup with co-solvents for the recovery of the whole electrolyte including the conducting salt. The latter two setups will be discussed in Section 6, here we concentrate on method (i): the shredded material is further processed by removing iron parts via a magnetic separation tool and then the electrode material is parted from the separator by air flow. The binder in the electrodes is removed by heating up to 400–600 °C which additionally causes the detachment of the current collectors from the active material particles. The graphite anode material and the copper and aluminum current collectors are taken out of the process and lithium is leached out of the cathode material, while the active material is dissolved in an acidic mixture. Several approaches are carried out to separate the heavy metals from each other: complexing agents such as di(2,4,4,trimethylpentyl)phosphinic acid [119]; or leaching with oxalate [120], ascorbic [121], citric [122] or concentrated acids [123–125]. However, biological approaches are also investigated [126]. The performance of the resynthesized cathode and anode material was reported by electrochemically and analytically characterized [127,128].

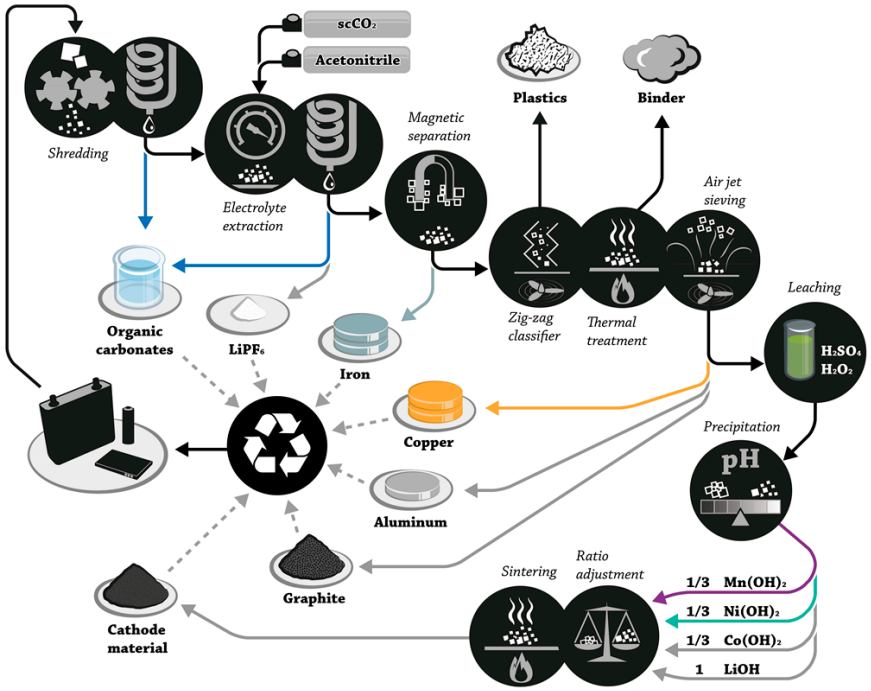

Figure 4. The mechanical-hydrometallurigcal "LithoRec II" recycling process. It was reproduced from reference [127], with permission from John Wiley & Sons 2016. $scCO_2$: supercritical carbon dioxide.

5. Carbon Dioxide and Its Extraction Properties

Besides being infamous as greenhouse gas [129–132], CO_2 is substantial to many chemical reactions. These reactions include the application as a monomer in materials synthesis [133] or as a C1 block in the fabrication of polycarbonates [134] or other organic compounds [135]. Furthermore, CO_2 is involved in the synthesis of linear and cyclic carbonates for LIB electrolytes as well [136–139]. It has been applied for lithium metal and lithium ion batteries as a SEI forming additive [140] and graphite anode surface modifications [141,142]. Additionally, due to the reduction or oxidation of the electrolyte CO_2 is produced and present in LIBs [143,144].

Aside from the standard phases (solid, liquid and gaseous), the supercritical phase is reached relatively non-elaborate. Temperature and pressure need to be increased above the critical point of 31 °C and 74 bar (Figure 5) [145]. In this state, supercritical CO_2 has the density of liquid CO_2 and the viscosity of gaseous CO_2. The physical properties are between those of the liquid and gaseous phase with greatly enhanced dissolution characteristics [146]. In combination with additional solvents, a wide variety of organic substances can be extracted and, therefore, supercritical carbon dioxide is the most applied supercritical medium for extraction [147]. It is normally used in food chemistry, with the well-known example of coffee decaffeination [148–152]. Other application areas include as a reaction medium for metal nanoparticle synthesis [153] or olefin polymerization [154], as a drying aid for electrode material synthesis [155] and crack-free silica aerogel production [156,157]. In supercritical fluid chromatography it functions as the eluent [147].

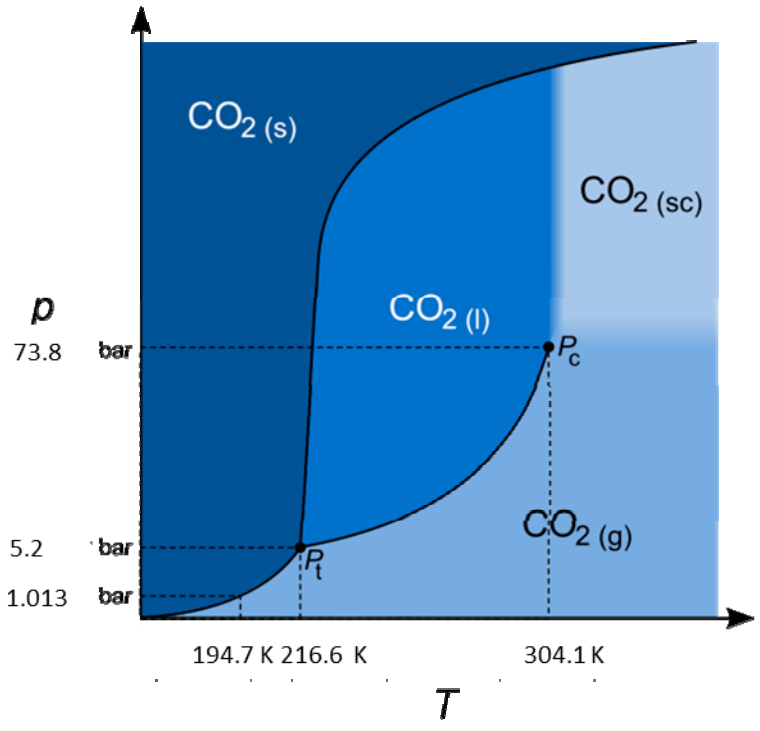

Figure 5. Pressure and temperature phase diagram of CO_2 [158,159]. K: Kelvin, p: pressure, T: temperature, sc: supercritical, l: liquid, g: gaseous, s: solid.

For supercritical extraction, commercial flow-through units with a corresponding compressor for the generation of supercritical CO_2 from liquid CO_2 are available. However, helium head pressure carbon dioxide ($HHPCO_2$) can be used as an alternative. Here, liquid carbon dioxide is compressed with a helium head pressure to 120 bar. Because of the different densities, in the two-phase system, supercritical carbon dioxide is available. Nevertheless, there are small deviations in the extraction behavior of $HHPCO_2$ compared to supercritical CO_2 due to little amounts of dissolved helium in the

CO_2 phase. This results in decreasing density of the helium head pressure carbon dioxide with reduced dissolving power towards aromatic analytes [160].

Nonetheless, compared to liquid solvent extraction, subcritical and supercritical CO_2 extraction offers unique advantages. The extraction is fast, highly selective and efficient. Furthermore, pre- or post-concentration or cleanup steps are not necessary [161].

6. Application of Subcritical and Supercritical CO_2 for Recycling of LIB Electrolytes

The use of CO_2 as an extraction medium was first mentioned in a patent by Sloop et al. Typical for a patent, the details about conditions and parameters as well as influence of the processing on the battery materials were not disclosed [115]. There are no further reports about any application of the patented process.

The first application of supercritical CO_2 for the extraction of LIB electrolytes was reported by Grützke et al., 2014 [19]. They applied supercritical helium head pressure carbon dioxide (scHHPCO_2) in an autoclave and investigated the extraction behavior with a set of two different separators and electrolytes (Figure 6). The extracts were analyzed by gas chromatography–mass spectrometry and ion chromatography–electrospray ionization–mass spectrometry to determine the recovery rate and the nature of the obtained electrolyte composition. It was stated that the recovery rates and extract compositions were strongly depending on the material of which the electrolyte was extracted. The highest achieved recovery rate was 73.5 ± 3.6 wt %.

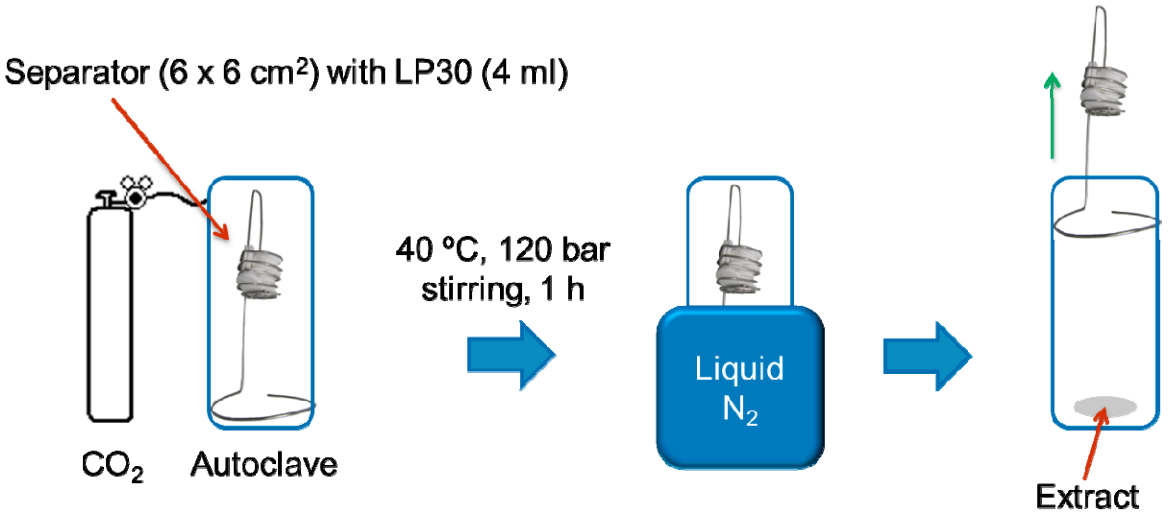

Figure 6. Schematic setup of the applied extraction procedure by Grützke et al. It was reproduced from reference [19] with permission from Elsevier, 2014.

After these proof-of-principle-experiments, commercial 18,650 cells were investigated as real samples. In addition to a reference cell, which was opened and extracted after formation, i.e., as supplied, LIB cells were electrochemically aged at 20 °C and 45 °C for post-mortem studies. The extracts were again analyzed by both mentioned techniques. Beside the electrolyte constituents, the following aging products were found and characterized: dimethyl-2,5-dioxahexane dicarboxylate (DMDOHC), ethylmethyl-2,5-dioxahexane dicarboxylate (EMDOHC) and diethyl-2,5-dioxahexane dicarboxylate (DEDOHC).

In all experiments, they showed the applicability of the CO_2 extraction. Furthermore, besides the application as a recycling tool, they showed the usefulness of the method for aging investigations on electrochemically treated cells. However, due to the obtained recovery rate, flow-through experiments with additional co-solvents were proposed in order to optimize the recovery rate.

Dai et al. described an alternative approach for the recovery of LIB electrolytes from separators with a commercial extraction system [162] (Figure 7). Fourier transform infrared spectroscopy (FT-IR), gas chromatography—mass spectrometry (GC-MS), ^{19}F- and ^{31}P-NMR and inductively

plasma–optical emission spectrometry (ICP-OES) were applied to systematically investigate the extract. The final recovery rate was determined as 85.07% ± 0.36%, however the conducting salt could not be recovered in sufficient amounts. They proposed that $LIPF_6$ was hydrolyzed during the supercritical CO_2 extraction process extraction, which was investigated with NMR to observe typical PF_6^- hydrolysis products. Furthermore, the extraction parameters were optimized by varying the operating parameters (extraction pressure, temperature and static time) according to the Box–Behnken design (Figure 8). With the help of a polynomial regression model, the mildest experimental conditions were determined (23.4 MPa, 40 °C and 45 min). The predicted recovery rate, 85.22%, was in very good agreement with the experimental recovery rate of 85.07%. Additionally, the results of the experiment showed that the extraction pressure is the major decisive factor for electrolyte extraction.

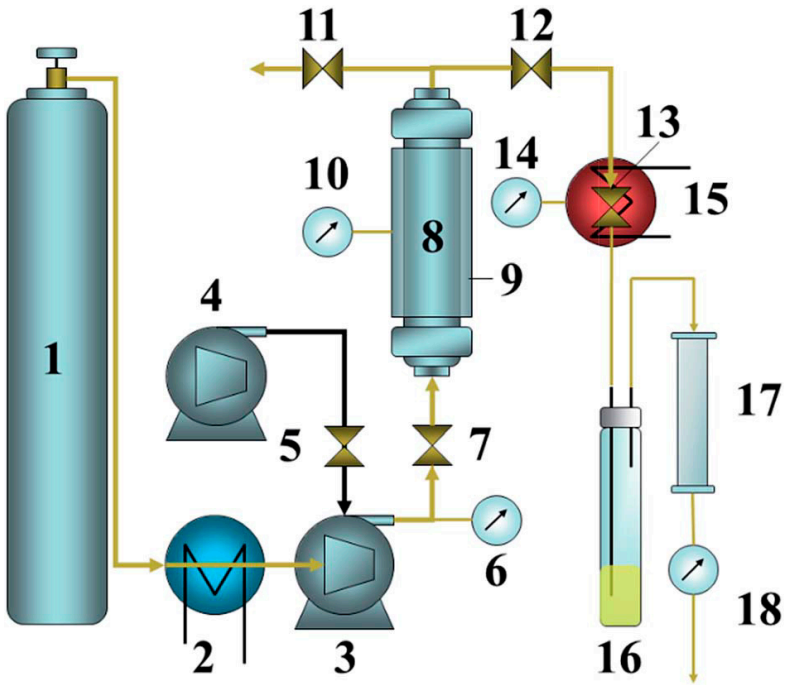

Figure 7. Schematic setup of the applied extraction procedure by Dai et al. with (1) CO_2 cylinder; (2) cooling bath; (3) air driven fluid pump (gas booster pump); (4) air compressor; (5) air regulator; (6) CO_2 pressure; (7) inlet valve; (8) extraction vessel; (9) heating jacket; (10) vessel heat; (11) vent valve; (12) outlet valve; (13) flow valve; (14) valve heat; (15) heating jacket; (16) collecting vial; (17) alumina filter; and (18) gas flow meter. It was reproduced from reference [162] with permission from the Royal Society of Chemistry, 2014.

In agreement with Grützke et al. [19], they emphasized the usefulness of supercritical CO_2 as an efficient and environment-friendly electrolyte separation method.

Following their static experiments, Grützke et al. applied a flow-through design [163]. They used supercritical and liquid carbon dioxide (sc and liq CO_2) under addition of different solvents for the optimized extraction of the electrolyte from commercial $LiNi_{0.33}Co_{0.33}Mn_{0.33}O_2$ (NMC))/graphite 18,650 cells (Figure 9). With 89.1 ± 3.4 wt %, the best overall recovery rate was achieved for the added ACN/PC mixture with the highest concentrations for EC and $LiPF_6$ (Figure 10). In addition, they investigated the time dependency of the recovered electrolyte for both setups. It was demonstrated that the developed method was suitable for LIB electrolyte extraction and post-mortem or aging investigations of LIB cell components because a qualitative overview was achieved after a few minutes of extraction also for apparently "dry" cells, where the electrolyte is deeply incorporated and immobilized in the electrode material.

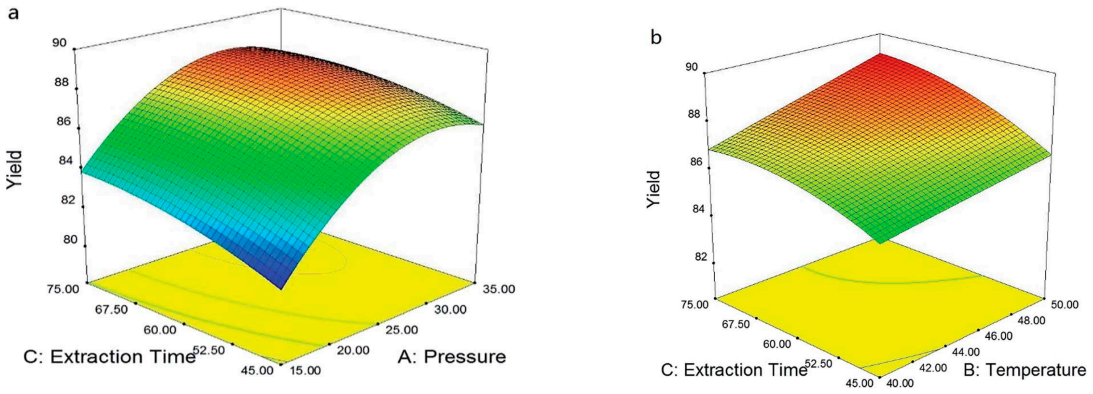

Figure 8. Response surfaces and contour plots for: (**a**) extraction time vs. pressure; and (**b**) extraction time vs. temperature. It was reproduced from reference [162] with permission from the Royal Society of Chemistry, 2014.

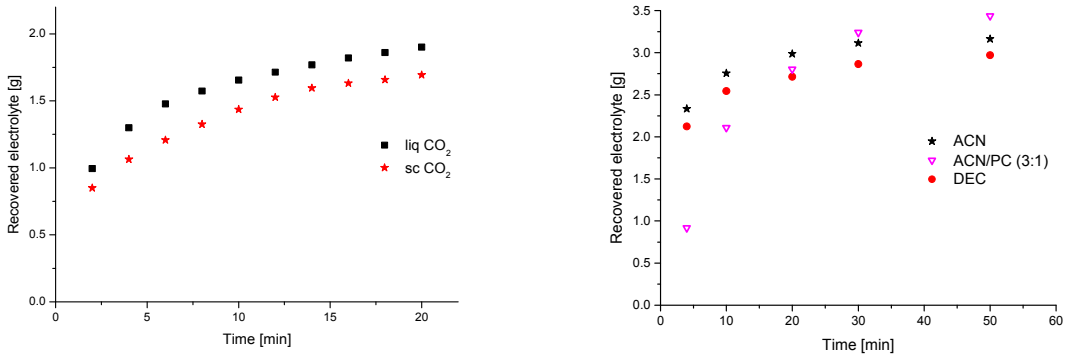

Figure 9. (**Left**) Time dependency of the amount of recovered electrolyte from commercial 18,650 cells after formation extracted with supercritical (300 bar, 40 °C; red stars) and liquid (60 bar, 25 °C; black squares) CO_2; and (**Right**) time dependency of the amount of recovered electrolyte from commercial 18,650 cells after formation extracted with liquid CO_2 and 0.5 mL/min additional solvents (black stars: acetonitrile (can); magenta triangles: ACN/propylene carbonate (PC) (3:1); red circles: diethyl carbonate (DEC)). It was reproduced from reference [163] with permission from the Royal Society of Chemistry, 2015.

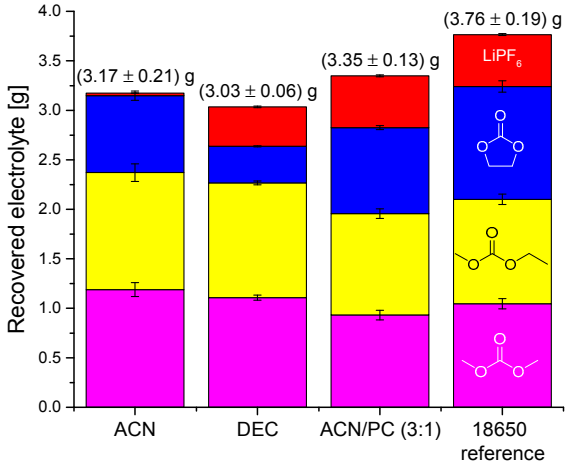

Figure 10. Compositions and amounts (determined with gas chromatography—mass spectrometry (GC-MS) and ion chromatography (IC)) of the recovered electrolytes from commercial 18,650 cells after formation extracted with liquid CO_2 and additional solvents for 30 min, with subsequent 20 min without additional solvent. Red, top: $LiPF_6$; blue, below: ethylene carbonate (EC); yellow, middle: ethyl methyl carbonate (EMC); magenta, bottom: dimethyl carbonate (DMC). It was reproduced from reference [163] with permission from the Royal Society of Chemistry, 2015.

In their second work on the topic, Dai et al. applied supercritical carbon dioxide as an extraction medium for the investigation of the extraction temperature and pressure (15 to 35 MPa), temperature (30 to 50 °C) [164]. The electrolytes were again adsorbed on a separator and investigated regarding the pressure (15–35 MPa), the temperature (30 to 50 °C) and the dynamical extraction time (25 to 65 min). Afterwards, the extract was analyzed with GC-FID (flame ionization detector) (Figures 11 and 12). The effect of the extraction pressure was examined using five levels from 15 to 35 MPa. The overall extraction yield was enhanced with higher pressures. This was attributed to the increased EC extraction yield under higher pressures due to the high polarity of supercritical CO_2.

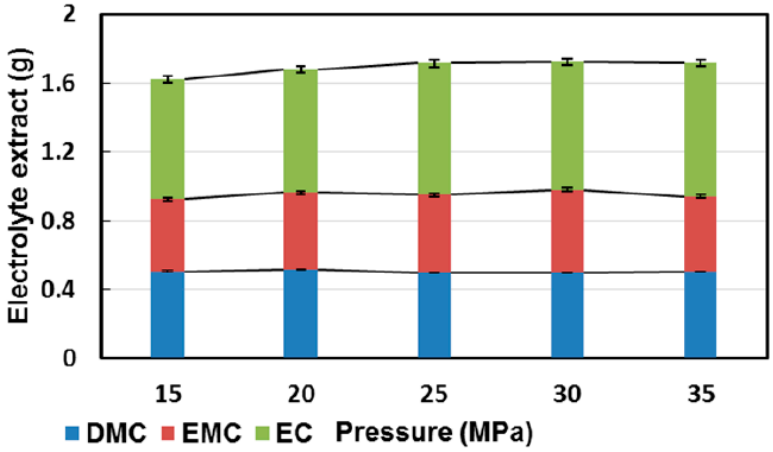

Figure 11. Compositions of the extracts corresponding to values obtained by gas chromatography—flame ionization detector (GC-FID) measurements. Green, top: EC; crimson, middle: EMC; blue, bottom: DMC [164].

The effect of temperature was investigated in a similar way (5 levels from 30 to 50 °C). Here, the temperature showed the same trend: with raising temperature, the overall extraction yield was increased. However, the extraction of EC was contradictory to the pressure experiments. The polarity of the supercritical carbon dioxide was reduced with higher temperatures; thus, Dai et al. [164] concluded that the polarity played a more important role than the supercritical fluid density.

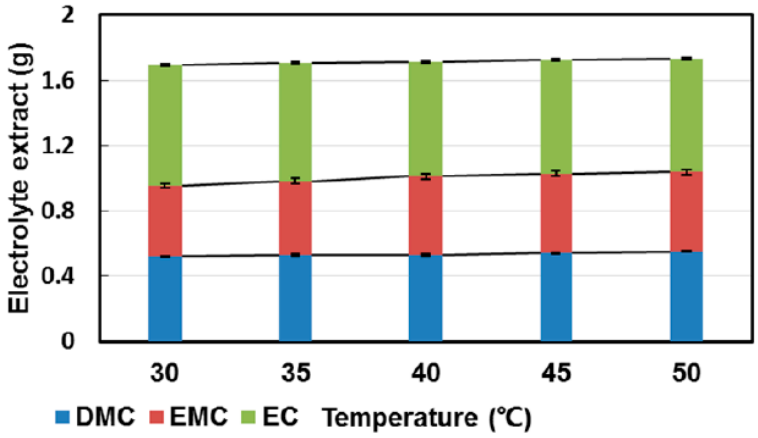

Figure 12. Compositions of the extracts corresponding to GC-FID measurements. Green, top: EC; crimson, middle: EMC; blue, bottom: DMC [164].

The overall highest recovery rate was reported as 88.71 ± 0.87 wt % but only in regard to the organic carbonate solvents. The conducting salt and aging products were not reported. As a conclusion of the extraction pressure and temperature experiments, they showed that the extraction process of carbonate is a predominantly determined by polarity. Furthermore, nonpolar carbonates should be extracted with non-polar or weakly polar extraction media. In comparison, polar carbonates

should be extracted with polar solvents or with the addition of medium polarity co-solvents into non-polar solvents.

Rothermel et al. applied the methods by Grützke et al. for the extraction of electrolytes and the subsequently effect on the graphite anode recycling efficiency [127]. Therefore, they applied three different approaches for their investigations: (i) thermal evaporation of volatile electrolyte components; (ii) electrolyte extraction with subcritical CO_2 and acetonitrile (ACN); and (iii) electrolyte extraction with supercritical CO_2. It should be noted that they replaced the term liquid CO_2 with subcritical CO_2 due to the fact that the used parameters were in fact subcritical and not liquid conditions for the CO_2. However, they concluded that the application of the supercritical carbon dioxide extraction method was unfavorable for the resulting crystallinity size of the graphite particles and therefore had an adverse impact on the electrochemical performance. In comparison, the electrolyte extraction using subcritical carbon dioxide was considered to be the "best" recycling method, as the recycled graphite showed the best electrochemical performance and the electrolyte was recovered by 90% including the conductive salt. In general, with the help of analytical and electrochemical characterization techniques it was shown that graphite originating from a previously electrochemically aged commercial cell subjected to a subcritical carbon dioxide assisted electrolyte in combination with a thermal treatment demonstrated the best electrochemical characteristics outperforming even fresh commercial synthetic graphite TIMREX® SLP50 which was used as benchmark (Table 2).

Table 2. Overview of the discharge capacities and associated Coulombic efficiencies obtained from electrochemical charge/discharge cycling experiments. $SubCO_2$: subcritical carbon dioxide. It was reprinted with permission from reference [127], Copyright John Wiley & Sons, 2016.

Sample (State of Health (SOH)	Coulombic Efficiency/%				Discharge Capacity 50th Cycle/mAh·g^{-1}
	1st Cycle	2nd Cycle	3rd Cycle	50th Cycle	
thermal (100%)	56.1 ± 1.8	91.8 ± 0.4	94.7 ± 0.3	99.8 ± 0.1	332.7 ± 0.3
thermal (70%)	85.4 ± 0.5	97.8 ± 0.3	98.5 ± 0.3	99.9 ± 0.1	346.8 ± 7.8
$subCO_2$ (100%)	81.6 ± 3.1	96.3 ± 1.2	97.6 ± 0.8	99.9 ± 0.1	372.7 ± 2.5
$subCO_2$ (70%)	82.9 ± 0.9	97.6 ± 0.1	98.5 ± 0.1	99.9 ± 0.1	379.9 ± 4.4
$scCO_2$ (100%)	78.7 ± 1.2	96.2 ± 0.4	97.4 ± 0.4	99.9 ± 0.1	348.8 ± 1.9
$scCO_2$ (70%)	82.0 ± 1.4	97.2 ± 0.3	98.2 ± 0.2	99.9 ± 0.1	375.0 ± 1.0
benchmark	84.8 ± 0.8	97.3 ± 0.2	98.2 ± 0.2	99.9 ± 0.1	357.6 ± 1.4

7. Application of Subcritical and Supercritical CO_2 as a Sample Preparation Tool

Besides minor aging investigations after supercritical or subcritical extraction (presented by Grützke et al. [19,104,163]) and the influence of the extraction method on the recyclability of graphite (reported by Rothermel et al. [127]), there is a recent study which focused primarily on aging investigations [165]. The aging experiments were conducted on commercial 18,650-type state-of-the-art cells to determine the influence of temperature during electrochemical cycling on the aging behavior of the different cell components. The cells, based on the $Li(Ni_{0.5}Co_{0.2}Mn_{0.3})O_2$/graphite chemistry, were aged at 20 °C and 45 °C to different states of health. The electrolyte was extracted based on the methods by Grützke et al. [19,163]. With the help of electrolyte aging analysis by GC-MS, it was shown, that temperature dependent cycling leads to differences in SEI composition. The electrolyte samples which were extracted with supercritical CO_2 from fresh and aged cells and revealed the following composition: the electrolyte of the fresh cell consisted of DMC and EC and PC as solvents, whereas fluoroethylene carbonate (FEC) [166] and succinonitrile [167] were identified as electrolyte additives in significant amounts. Furthermore, traces of vinylene carbonate (VC) [75] and 1,3-propane sultone [168] were detected in the electrolyte (Figure 13). The cell aged at 45 °C shows traces of FEC in the electrolyte after more than 1000 cycles. In contrast, the additive FEC was no longer detected in the cells cycled at 20 °C. With the help of the supercritical CO_2 extraction, which made even traces of electrolyte additives and decomposition products available, they could conclude that after FEC

consumption, the amount of organic SEI components increased and PC could co-intercalate, thus leading to a poorer performing SEI for the cells cycled at 20 °C compared to those cells at 45 °C.

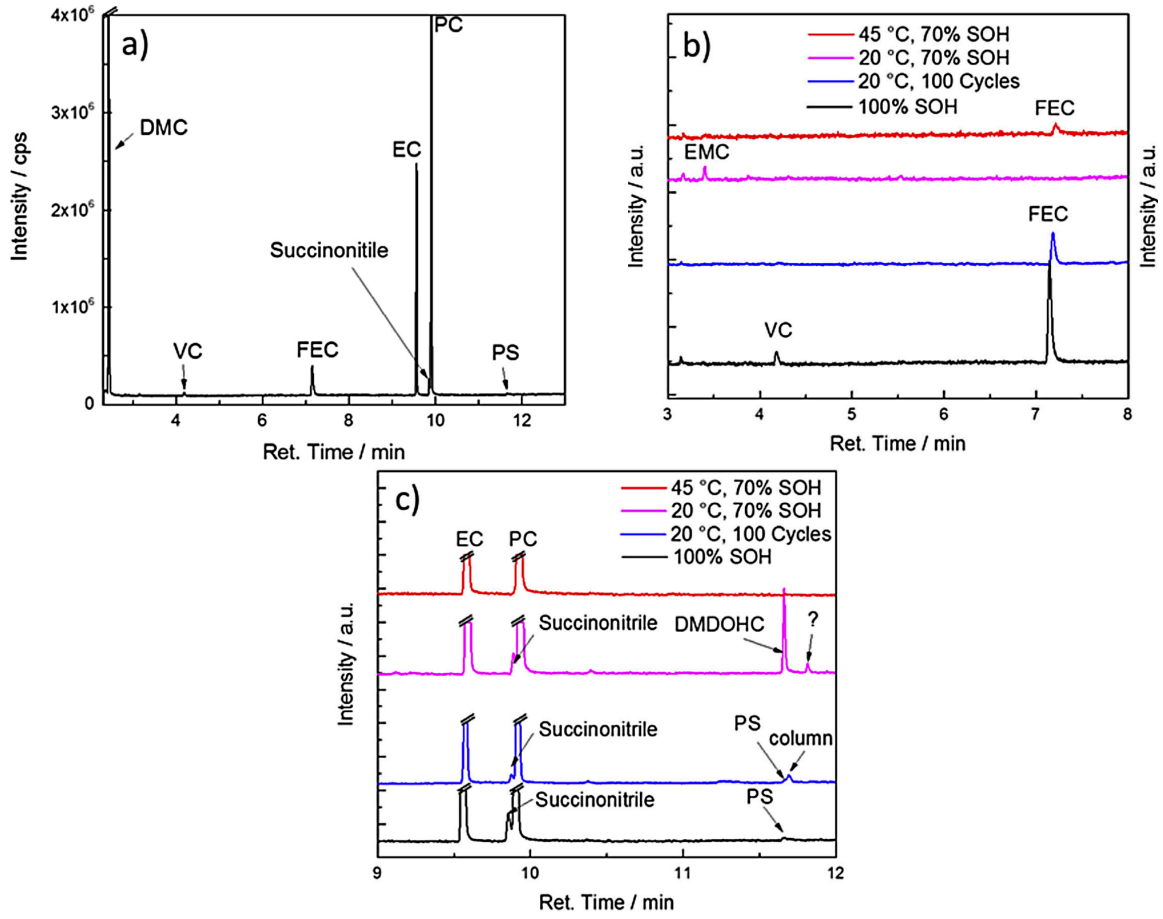

Figure 13. GC-MS investigations on the electrolyte of a fresh cell extracted with supercritical CO_2 (**a**); and comparisons of fresh and aged electrolytes at significant retention times (**b**,**c**). It was reproduced from reference [165] with permission from Elsevier, 2017.

8. Conclusions

Contrary to previous reports, the role of CO_2 as an extraction medium is important in general and very promising for future applications as LIB cell extraction. For the sake of more refined post-mortem and aging analyses of LIB cell components, the quantitative extraction with subcritical/liquid and supercritical CO_2 holds the advantage that there is no loss of information due to dilution factors (which occurs with regular solvents) or by missing compounds that could not be extracted due to polarity/non-polarity of the target compounds.

Since the numbers of used portable consumer products rise enormously and, more important, xEVs are penetrating the market in greater and greater quantities, new strategies are needed. Especially recycling, as growing application and research field in a holistic treatment of lithium ion batteries relies on novel, more effective and efficient process techniques such as CO_2 extraction. Together with a strict legislation on the recycling rate and the decreasing availability of the raw battery materials, the enormous growth rates in used LIBs will become most significant for further growth in importance of this processing technique.

Acknowledgments: We kindly acknowledge the Federal Ministry of Education and Research for funding the Project Elektrolytlabor (project grant number: 03X4632) and the Federal Ministry for the Environment, Nature Conservation and Nuclear Safety for funding of the project LithoRec II (project grant number: 16EM1025).

Author Contributions: S.N. wrote the paper with input and editing from M.W.

Conflicts of Interest: The authors declare no conflict of interest.

References

1. Wagner, R.; Preschitschek, N.; Passerini, S.; Leker, J.; Winter, M. Current research trends and prospects among the various materials and designs used in lithium-based batteries. *J. Appl. Electrochem.* **2013**, *43*, 481–496.
2. Winter, M.; Brodd, R.J. What Are Batteries, Fuel Cells, and Supercapacitors? *Chem. Rev.* **2004**, *104*, 4245–4270.
3. Bieker, P.; Winter, M. Lithium-Ionen-Technologie und was danach kommen könnte. *Chem. Unserer Zeit* **2016**, *50*, 172–186.
4. Meister, P.; Jia, H.; Li, J.; Kloepsch, R.; Winter, M.; Placke, T. Best Practice: Performance and Cost Evaluation of Lithium Ion Battery Active Materials with Special Emphasis on Energy Efficiency. *Chem. Mater.* **2016**, *28*, 7203–7217.
5. Current Calendar Year Monthly Average Settlement Prices (30 June 2015). The London Metal Exchange Limited. London, UK. Available online: http://www.lme.com/~/media/Files/Market%20data/Historic%20Data/2015/June%202015.xlsx (accessed on 2 April 2016).
6. Sonoc, A.; Jeswiet, J. A Review of Lithium Supply and Demand and a Preliminary Investigation of a Room Temperature Method to Recycle Lithium Ion Batteries to Recover Lithium and Other Materials. *Procedia CIRP* **2014**, *15*, 289–293.
7. Reuter, M.; Hudson, C.; Van Schaik, A.; Heiskanen, K.; Meskers, C.; Hagelüken, C. *Metal Recycling: Opportunities, Limits, Infrastructure*; United Nations Environment Programme: Paris, France, 2013; pp. 1–320.
8. Gruber, P.W.; Medina, P.A.; Keoleian, G.A.; Kesler, S.E.; Everson, M.P.; Wallington, T.J. Global lithium availability. *J. Ind. Ecol.* **2011**, *15*, 760–775.
9. Perez, A.A.; Safirova, E.; Anderson, S.T. *The Mineral Industries of Europe and Central Eurasia*; U.S. Geological Survey: Reston, VA, USA, 2014; pp. 1–34.
10. Battery-Kutter News. Available online: https://www.battery-kutter.de/main/news_detail&nid=52 (accessed on 28 January 2017).
11. *Directive 2006/66/EC on Batteries and Accumulators and Waste Batteries and Accumulators*; The European Parliament and the Council of the European Union: Brussels, Belgium, 2006; Volume L 266/1.
12. *Directive 2012/19/EU on Waste Electrical and Electronic Equipment (WEEE)*; The European Parliament and the Council of the European Union: Brussels, Belgium, 2012; Volume L 197/38.
13. *Directive 2000/53/EC on End-of Life Vehicles*; The European Parliament and the Council of the European Union: Brussels, Belgium, 2000; Volume L 269/34.
14. Vetter, J.; Novák, P.; Wagner, M.; Veit, C.; Möller, K.-C.; Besenhard, J.; Winter, M.; Wohlfahrt-Mehrens, M.; Vogler, C.; Hammouche, A. Ageing mechanisms in lithium-ion batteries. *J. Power Sources* **2005**, *147*, 269–281.
15. Garche, J.; Dyer, C.K.; Moseley, P.T.; Ogumi, Z.; Rand, D.A.; Scrosati, B. *Encyclopedia of Electrochemical Power Sources*, 1 ed.; Elsevier Science: Amsterdam, the Netherlands, 2013; p. 4538.
16. Börner, M.; Friesen, A.; Grützke, M.; Stenzel, Y.; Brunklaus, G.; Haetge, J.; Nowak, S.; Schappacher, F.; Winter, M. Correlation of aging and thermal stability of commercial 18650-type lithium ion batteries. *J. Power Sources* **2017**, *342*, 382–392.
17. Grützke, M.; Kraft, V.; Hoffmann, B.; Klamor, S.; Diekmann, J.; Kwade, A.; Winter, M.; Nowak, S. Aging investigations of a lithium-ion battery electrolyte from a field-tested hybrid electric vehicle. *J. Power Sources* **2015**, *273*, 83–88.
18. Kraft, V.; Grützke, M.; Weber, W.; Menzel, J.; Wiemers-Meyer, S.; Winter, M.; Nowak, S. Two-dimensional ion chromatography for the separation of ionic organophosphates generated in thermally decomposed lithium hexafluorophosphate-based lithium ion battery electrolytes. *J. Chromatogr. A* **2015**, *1409*, 201–209.
19. Grützke, M.; Kraft, V.; Weber, W.; Wendt, C.; Friesen, A.; Klamor, S.; Winter, M.; Nowak, S. Supercritical carbon dioxide extraction of lithium-ion battery electrolytes. *J. Supercrit. Fluids* **2014**, *94*, 216–222.
20. Fleischhammer, M.; Waldmann, T.; Bisle, G.; Hogg, B.-I.; Wohlfahrt-Mehrens, M. Interaction of cyclic ageing at high-rate and low temperatures and safety in lithium-ion batteries. *J. Power Sources* **2015**, *274*, 432–439.
21. Gachot, G.; Grugeon, S.; Eshetu, G.G.; Mathiron, D.; Ribière, P.; Armand, M.; Laruelle, S. Thermal behaviour of the lithiated-graphite/electrolyte interface through GC/MS analysis. *Electrochim. Acta* **2012**, *83*, 402–409.

22. Krueger, S.; Kloepsch, R.; Li, J.; Nowak, S.; Passerini, S.; Winter, M. How do reactions at the anode/electrolyte interface determine the cathode performance in lithium-ion batteries? *J. Electrochem. Soc.* **2013,** 160, A542–A548.
23. Börner, M.; Klamor, S.; Hoffmann, B.; Schroeder, M.; Nowak, S.; Würsig, A.; Winter, M.; Schappacher, F. Investigations on the C-Rate and Temperature Dependence of Manganese Dissolution/Deposition in $LiMn_2O_4/Li_4Ti_5O_{12}$ Lithium Ion Batteries. *J. Electrochem. Soc.* **2016,** *163*, A831–A837.
24. Jung, S.K.; Gwon, H.; Hong, J.; Park, K.Y.; Seo, D.H.; Kim, H.; Hyun, J.; Yang, W.; Kang, K. Understanding the degradation mechanisms of $LiNi_{0.5}Co_{0.2}Mn_{0.3}O_2$ cathode material in lithium ion batteries. *Adv. Energy Mater.* **2014**, *4*, doi:10.1002/aenm.201300787.
25. Winter, M. The solid electrolyte interphase—The most important and the least understood solid electrolyte in rechargeable Li batteries. *Z. Phys. Chem. Int. J. Res. Phys. Chem. Chem. Phys.* **2009**, *223*, 1395–1406.
26. Peled, E. The electrochemical behavior of alkali and alkaline earth metals in nonaqueous battery systems—The solid electrolyte interphase model. *J. Electrochem. Soc.* **1979**, *126*, 2047–2051.
27. Agubra, V.A.; Fergus, J.W.; Fu, R.; Choe, S.-Y. Analysis of effects of the state of charge on the formation and growth of the deposit layer on graphite electrode of pouch type lithium ion polymer batteries. *J. Power Sources* **2014**, *270*, 213–220.
28. Chung, G.C.; Kim, H.J.; Yu, S.I.; Jun, S.H.; Choi, J.W.; Kim, M.H. Origin of graphite exfoliation an investigation of the important role of solvent cointercalation. *J. Electrochem. Soc.* **2000**, *147*, 4391–4398.
29. Klett, M.; Svens, P.; Tengstedt, C.; Seyeux, A.; Światowska, J.; Lindbergh, G.R.; Wreland Lindström, R. Uneven film formation across depth of porous graphite electrodes in cycled commercial Li-ion batteries. *J. Phys. Chem. C* **2014,** *119*, 90–100.
30. Wiemers-Meyer, S.; Jeremias, S.; Winter, M.; Nowak, S. Influence of Battery Cell Components and Water on the Thermal and Chemical Stability of LiPF 6 Based Lithium Ion Battery Electrolytes. *Electrochim. Acta* **2016**, *222*, 1267–1271.
31. Niehoff, P.; Kraemer, E.; Winter, M. Parametrisation of the influence of different cycling conditions on the capacity fade and the internal resistance increase for lithium nickel manganese cobalt oxide/graphite cells. *J. Electroanal. Chem.* **2013**, *707*, 110–116.
32. Friesen, A.; Schultz, C.; Brunklaus, G.; Rodehorst, U.; Wilken, A.; Haetge, J.; Winter, M.; Schappacher, F. Long Term Aging of Automotive Type Lithium-Ion Cells. *ECS Trans.* **2015**, *69*, 89–99.
33. Friesen, A.; Horsthemke, F.; Mönnighoff, X.; Brunklaus, G.; Krafft, R.; Börner, M.; Risthaus, T.; Winter, M.; Schappacher, F.M. Impact of cycling at low temperatures on the safety behavior of 18650-type lithium ion cells: Combined study of mechanical and thermal abuse testing accompanied by *post-mortem* analysis. *J. Power Sources* **2016**, *334*, 1–11.
34. Lux, S.F.; Chevalier, J.; Lucas, I.T.; Kostecki, R. HF Formation in LiPF6-Based Organic Carbonate Electrolytes. *ECS Electrochem. Lett.* **2013,** 2, A121–A123.
35. Terborg, L.; Nowak, S.; Passerini, S.; Winter, M.; Karst, U.; Haddad, P.R.; Nesterenko, P.N. Ion chromatographic determination of hydrolysis products of hexafluorophosphate salts in aqueous solution. *Anal. Chim. Acta* **2012**, *714*, 121–126.
36. Terborg, L.; Weber, S.; Blaske, F.; Passerini, S.; Winter, M.; Karst, U.; Nowak, S. Investigation of thermal aging and hydrolysis mechanisms in commercial lithium ion battery electrolyte. *J. Power Sources* **2013**, *242*, 832–837.
37. Handel, P.; Fauler, G.; Kapper, K.; Schmuck, M.; Stangl, C.; Fischer, R.; Uhlig, F.; Koller, S. Thermal aging of electrolytes used in lithium-ion batteries—An investigation of the impact of protic impurities and different housing materials. *J. Power Sources* **2014**, *267*, 255–259.
38. Yang, H.; Zhuang, G.V.; Ross, P.N. Thermal stability of LiPF 6 salt and Li-ion battery electrolytes containing LiPF 6. *J. Power Sources* **2006**, *161*, 573–579.
39. Pyschik, M.; Klein-Hitpaß, M.; Girod, S.; Winter, M.; Nowak, S. Capillary electrophoresis with contactless conductivity detection for the quantification of fluoride in lithium ion battery electrolytes and in ionic liquids—A comparison to the results gained with a fluoride ion-selective electrode. *Electrophoresis* **2016**, doi:10.1002/elps.201600361.
40. Wilken, A.; Kraft, V.; Girod, S.; Winter, M.; Nowak, S. A fluoride-selective electrode (Fse) for the quantification of fluoride in lithium-ion battery (Lib) electrolytes. *Anal. Methods* **2016**, *8*, 6932–6940.

41. Campion, C.L.; Li, W.; Euler, W.B.; Lucht, B.L.; Ravdel, B.; DiCarlo, J.F.; Gitzendanner, R.; Abraham, K. Suppression of toxic compounds produced in the decomposition of lithium-ion battery electrolytes. *Electrochem. Solid-State Lett.* **2004**, *7*, A194–A197.
42. Campion, C.L.; Li, W.; Lucht, B.L. Thermal decomposition of LiPF6-based electrolytes for lithium-ion batteries. *J. Electrochem. Soc.* **2005,** 152, A2327–A2334.
43. Kraft, V.; Grützke, M.; Weber, W.; Winter, M.; Nowak, S. Ion chromatography electrospray ionization mass spectrometry method development and investigation of lithium hexafluorophosphate-based organic electrolytes and their thermal decomposition products. *J. Chromatogr. A* **2014**, *1354*, 92–100.
44. Vortmann, B.; Nowak, S.; Engelhard, C. Rapid characterization of lithium ion battery electrolytes and thermal aging products by low-temperature plasma ambient ionization high-resolution mass spectrometry. *Anal. Chem.* **2013**, *85*, 3433–3438.
45. Weber, W.; Kraft, V.; Grützke, M.; Wagner, R.; Winter, M.; Nowak, S. Identification of alkylated phosphates by gas chromatography–mass spectrometric investigations with different ionization principles of a thermally aged commercial lithium ion battery electrolyte. *J. Chromatogr. A* **2015**, *1394*, 128–136.
46. Weber, W.; Wagner, R.; Streipert, B.; Kraft, V.; Winter, M.; Nowak, S. Ion and gas chromatography mass spectrometry investigations of organophosphates in lithium ion battery electrolytes by electrochemical aging at elevated cathode potentials. *J. Power Sources* **2016**, *306*, 193–199.
47. Kraft, V.; Weber, W.; Grützke, M.; Winter, M.; Nowak, S. Study of decomposition products by gas chromatography-mass spectrometry and ion chromatography-electrospray ionization-mass spectrometry in thermally decomposed lithium hexafluorophosphate-based lithium ion battery electrolytes. *RSC Adv.* **2015**, *5*, 80150–80157.
48. Kraft, V.; Weber, W.; Streipert, B.; Wagner, R.; Schultz, C.; Winter, M.; Nowak, S. Qualitative and quantitative investigation of organophosphates in an electrochemically and thermally treated lithium hexafluorophosphate-based lithium ion battery electrolyte by a developed liquid chromatography-tandem quadrupole mass spectrometry method. *RSC Adv.* **2016**, *6*, 8–17.
49. Ravdel, B.; Abraham, K.; Gitzendanner, R.; DiCarlo, J.; Lucht, B.; Campion, C. Thermal stability of lithium-ion battery electrolytes. *J. Power Sources* **2003**, *119*, 805–810.
50. Gachot, G. g.; Ribière, P.; Mathiron, D.; Grugeon, S.; Armand, M.; Leriche, J.-B.; Pilard, S.; Laruelle, S.P. Gas chromatography/mass spectrometry as a suitable tool for the Li-ion battery electrolyte degradation mechanisms study. *Anal. Chem.* **2010**, *83*, 478–485.
51. Schultz, C.; Kraft, V.; Pyschik, M.; Weber, S.; Schappacher, F.; Winter, M.; Nowak, S. Separation and quantification of organic electrolyte components in lithium-ion batteries via a developed HPLC method. *J. Electrochem. Soc.* **2015**, *162*, A629–A634.
52. Schultz, C.; Vedder, S.; Winter, M.; Nowak, S. Qualitative Investigation of the Decomposition of Organic Solvent Based Lithium Ion Battery Electrolytes with LC-IT-TOF-MS. *Anal. Chem.* **2016**, *88*, 11160–11168.
53. Grützke, M.; Weber, W.; Winter, M.; Nowak, S. Structure determination of organic aging products in lithium-ion battery electrolytes with gas chromatography chemical ionization mass spectrometry (GC-CI-MS). *RSC Adv.* **2016**, *6*, 57253–57260.
54. Terborg, L.; Weber, S.; Passerini, S.; Winter, M.; Karst, U.; Nowak, S. Development of gas chromatographic methods for the analyses of organic carbonate-based electrolytes. *J. Power Sources* **2014**, *245*, 836–840.
55. Wiemers-Meyer, S.; Winter, M.; Nowak, S. Mechanistic insights into lithium ion battery electrolyte degradation—A quantitative NMR study. *Phys. Chem. Chem. Phys.* **2016**, *18*, 26595–26601.
56. Wiemers-Meyer, S.; Winter, M.; Nowak, S. Battery Cell for In Situ NMR Measurements of Liquid Electrolytes. *Phys. Chem. Chem. Phys.* **2017**, *19*, 4962–4966.
57. Abraham, K. Directions in secondary lithium battery research and development. *Electrochim. Acta* **1993**, *38*, 1233–1248.
58. Balbuena, P.B.; Wang, Y. *Lithium-Ion Batteries: Solid-Electrolyte Interphase*; World Scientific: Singapore, 2004; p. 424.
59. Jow, T.R.; Xu, K.; Borodin, O.; Makoto, U. *Electrolytes for Lithium and Lithium-Ion Batteries*; Springer: Berlin, Germany, 2014; Volum 58.
60. Xu, K. Electrolytes and interphases in Li-ion batteries and beyond. *Chem. Rev.* **2014**, *114*, 11503–11618.
61. Xu, K. Nonaqueous liquid electrolytes for lithium-based rechargeable batteries. *Chem. Rev.* **2004**, *104*, 4303–4418.

62. Schmitz, R.W.; Murmann, P.; Schmitz, R.; Müller, R.; Krämer, L.; Kasnatscheew, J.; Isken, P.; Niehoff, P.; Nowak, S.; Röschenthaler, G.-V. Investigations on novel electrolytes, solvents and SEI additives for use in lithium-ion batteries: Systematic electrochemical characterization and detailed analysis by spectroscopic methods. *Prog. Solid State Chem.* **2014**, *42*, 65–84.
63. Tasaki, K.; Goldberg, A.; Winter, M. On the difference in cycling behaviors of lithium-ion battery cell between the ethylene carbonate-and propylene carbonate-based electrolytes. *Electrochim. Acta* **2011**, *56*, 10424–10435.
64. Wakihara, M.; Yamamoto, O. *Lithium Ion Batteries: Fundamentals and Performance*; John Wiley & Sons: Hoboken, NJ, USA, 2008.
65. Aurbach, D.; Talyosef, Y.; Markovsky, B.; Markevich, E.; Zinigrad, E.; Asraf, L.; Gnanaraj, J.S.; Kim, H.-J. Design of electrolyte solutions for Li and Li-ion batteries: A review. *Electrochim. Acta* **2004**, *50*, 247–254.
66. Krämer, E.; Passerini, S.; Winter, M. Dependency of aluminum collector corrosion in lithium ion batteries on the electrolyte solvent. *ECS Electrochem. Lett.* **2012**, *1*, C9–C11.
67. Newman, G.; Francis, R.; Gaines, L.; Rao, B. Hazard investigations of LiClO4/dioxolane electrolyte. *J. Electrochem. Soc.* **1980**, *127*, 2025–2027.
68. Ding, M.S.; Xu, K.; Jow, T.R. Conductivity and Viscosity of PC-DEC and PC-EC Solutions of LiBOB. *J. Electrochem. Soc.* **2005**, *152*, A132–A140.
69. Amereller, M.; Schedlbauer, T.; Moosbauer, D.; Schreiner, C.; Stock, C.; Wudy, F.; Zugmann, S.; Hammer, H.; Maurer, A.; Gschwind, R. Electrolytes for lithium and lithium ion batteries: From synthesis of novel lithium borates and ionic liquids to development of novel measurement methods. *Prog. Solid State Chem.* **2014**, *42*, 39–56.
70. Rupp, B.; Schmuck, M.; Balducci, A.; Winter, M.; Kern, W. Polymer electrolyte for lithium batteries based on photochemically crosslinked poly(ethylene oxide) and ionic liquid. *Eur. Polym. J.* **2008**, *44*, 2986–2990.
71. Zhang, S.S. A review on electrolyte additives for lithium-ion batteries. *J. Power Sources* **2006**, *162*, 1379–1394.
72. Shigematsu, Y.; Kinoshita, S.-I.; Ue, M. Thermal behavior of a C/$LiCoO_2$ cell, its components, and their combinations and the effects of electrolyte additives. *J. Electrochem. Soc.* **2006**, *153*, A2166–A2170.
73. Tobishima, S.; Ogino, Y.; Watanabe, Y. Influence of electrolyte additives on safety and cycle life of rechargeable lithium cells. *J. Appl. Electrochem.* **2003**, *33*, 143–150.
74. Möller, K.-C.; Santner, H.; Kern, W.; Yamaguchi, S.; Besenhard, J.; Winter, M. In situ characterization of the SEI formation on graphite in the presence of a vinylene group containing film-forming electrolyte additives. *J. Power Sources* **2003**, *119*, 561–566.
75. Santner, H.; Korepp, C.; Winter, M.; Besenhard, J.; Möller, K.-C. In-situ FTIR investigations on the reduction of vinylene electrolyte additives suitable for use in lithium-ion batteries. *Anal. Bioanal. Chem.* **2004**, *379*, 266–271.
76. Vogl, U.; Schmitz, A.; Stock, C.; Badillo, J.P.; Gores, H.J.; Winter, M. Investigation of N-ethyl-2-pyrrolidone (NEP) as electrolyte additive in regard to overcharge protecting characteristics. *J. Electrochem. Soc.* **2014,** *161*, A1407–A1414.
77. Dippel, C.; Schmitz, R.; Müller, R.; Böttcher, T.; Kunze, M.; Lex-Balducci, A.; Röschenthaler, G.-V.; Passerini, S.; Winter, M. Carbene Adduct as Overcharge Protecting Agent in Lithium Ion Batteries. *J. Electrochem. Soc.* **2012**, *159*, A1587–A1590.
78. Korepp, C.; Kern, W.; Lanzer, E.; Raimann, P.; Besenhard, J.; Yang, M.; Möller, K.-C.; Shieh, D.-T.; Winter, M. 4-Bromobenzyl isocyanate versus benzyl isocyanate—New film-forming electrolyte additives and overcharge protection additives for lithium ion batteries. *J. Power Sources* **2007**, *174*, 637–642.
79. Schranzhofer, H.; Bugajski, J.; Santner, H.; Korepp, C.; Möller, K.-C.; Besenhard, J.; Winter, M.; Sitte, W. Electrochemical impedance spectroscopy study of the SEI formation on graphite and metal electrodes. *J. Power Sources* **2006**, *153*, 391–395.
80. Dey, A. Lithium anode film and organic and inorganic electrolyte batteries. *Thin Solid Films* **1977**, *43*, 131–171.
81. Peled, E.; Yamin, H. Kinetics of Lithium in Lithium $LiAlCl_4$-$SoCl_2$ Solutions; *J. Electrochem. Soc.* **1979**, C308.
82. Dupré, N.; Martin, J.-F.; Degryse, J.; Fernandez, V.; Soudan, P.; Guyomard, D. Aging of the LiFePO 4 positive electrode interface in electrolyte. *J. Power Sources* **2010**, *195*, 7415–7425.
83. Kong, W.; Li, H.; Huang, X.; Chen, L. Gas evolution behaviors for several cathode materials in lithium-ion batteries. *J. Power Sources* **2005,** *142*, 285–291.

84. Sloop, S.E.; Kerr, J.B.; Kinoshita, K. The role of Li-ion battery electrolyte reactivity in performance decline and self-discharge. *J. Power Sources* **2003**, *119*, 330–337.
85. Sloop, S.E.; Pugh, J.K.; Wang, S.; Kerr, J.; Kinoshita, K. Chemical Reactivity of PF 5 and LiPF6 in Ethylene Carbonate/Dimethyl Carbonate Solutions. *Electrochem. Solid-State Lett.* **2001,** *4*, A42–A44.
86. Wilken, S.; Treskow, M.; Scheers, J.; Johansson, P.; Jacobsson, P. Initial stages of thermal decomposition of LiPF 6-based lithium ion battery electrolytes by detailed Raman and NMR spectroscopy. *RSC Adv.* **2013**, *3*, 16359–16364.
87. Kawamura, T.; Okada, S.; Yamaki, J.-i. Decomposition reaction of LiPF 6-based electrolytes for lithium ion cells. *J. Power Sources* **2006**, *156*, 547–554.
88. Plakhotnyk, A.V.; Ernst, L.; Schmutzler, R. Hydrolysis in the system LiPF 6—Propylene Carbonate—dimethyl carbonate—H_2O. *J. Fluorine Chem.* **2005**, *126*, 27–31.
89. Blomgren, G.E. Electrolytes for advanced batteries. *J. Power Sources* **1999**, *81*, 112–118.
90. Sasaki, T.; Abe, T.; Iriyama, Y.; Inaba, M.; Ogumi, Z. Formation mechanism of alkyl dicarbonates in Li-ion cells. *J. Power Sources* **2005**, *150*, 208–215.
91. Sasaki, T.; Jeong, S.-K.; Abe, T.; Iriyama, Y.; Inaba, M.; Ogumi, Z. Effect of an alkyl dicarbonate on Li-ion cell performance. *J. Electrochem. Soc.* **2005,** *152*, A1963-A1968.
92. Silver, S. The Toxieity of Dimethyl-, Diethyl-, and Diisopropyl Fluorophosphate Vapors. *J. Ind. Hyg. Toxicol.* **1948**, *30*, 307–311.
93. Tripathi, H.L.; Dewey, W.L. Comparison of the effects of diisopropylfluorophosphate, sarin, soman, and tabun on toxicity and brain acetylcholinesterase activity in mice. *J. Toxicol. Environ. Health Part A* **1989**, *26*, 437–446.
94. Referenced to Journal of Toxicology and Environmental Health 1989, 26, 437. Available online: www.lookchem.com (accessed on 28 April 2017).
95. Referenced to NTIS (National Technical Information Service). Available online: www.lookchem.com (accessed on 28 April 2017).
96. Referenced to Deutsche Gesundheitswesen 1960, 15, 2179. Available online: www.lookchem.com (accessed on 28 April 2017).
97. Referenced to RTECS (Registry of Toxic Effects of Chemical Substances). Available online: www.sigmaaldrich.com (accessed on 28 April 2017).
98. TOXNET Database. Available online: https://toxnet.nlm.nih.gov/ (accessed on 10 September 2016).
99. Patnaik, P. *A Comprehensive Guide to the Hazardous Properties of Chemical Substances*; John Wiley & Sons: Hoboken, NJ, USA, 2007.
100. Delfino, R.T.; Ribeiro, T.S.; Figueroa-Villar, J.D. Organophosphorus compounds as chemical warfare agents: A review. *J. Braz. Chem. Soc.* **2009**, *20*, 407–428.
101. Copplestone, J.F. The development of the WHO Recommended Classification of Pesticides by Hazard. *Bull. World Health Org.* **1988**, *66*, 545.
102. Raushel, F.M. Chemical biology: Catalytic detoxification. *Nature* **2011**, *469*, 310–311.
103. Costa, L.G. Current issues in organophosphate toxicology. *Clin. Chim. Acta* **2006**, *366*, 1–13.
104. Grützke, M.; Krüger, S.; Kraft, V.; Vortmann, B.; Rothermel, S.; Winter, M.; Nowak, S. Investigation of the Storage Behavior of Shredded Lithium-Ion Batteries from Electric Vehicles for Recycling Purposes. *ChemSusChem* **2015**, *8*, 3433–3438.
105. Zhang, P.; Yokoyama, T.; Itabashi, O.; Suzuki, T.M.; Inoue, K. Hydrometallurgical process for recovery of metal values from spent lithium-ion secondary batteries. *Hydrometallurgy* **1998,** *47*, 259–271.
106. Freitas, M.; Garcia, E. Electrochemical recycling of cobalt from cathodes of spent lithium-ion batteries. *J. Power Sources* **2007**, *171*, 953–959.
107. Swain, B.; Jeong, J.; Lee, J.-C.; Lee, G.-H.; Sohn, J.-S. Hydrometallurgical process for recovery of cobalt from waste cathodic active material generated during manufacturing of lithium ion batteries. *J. Power Sources* **2007**, *167*, 536–544.
108. Lain, M.J. Recycling of lithium ion cells and batteries. *J. Power Sources* **2001**, *97*, 736–738.
109. Georgi-Maschler, T.; Friedrich, B.; Weyhe, R.; Heegn, H.; Rutz, M. Development of a recycling process for Li-ion batteries. *J. Power Sources* **2012**, *207*, 173–182.
110. Contestabile, M.; Panero, S.; Scrosati, B. A laboratory-scale lithium-ion battery recycling process. *J. Power Sources* **2001**, *92*, 65–69.

111. Castillo, S.; Ansart, F.; Laberty-Robert, C.; Portal, J. Advances in the recovering of spent lithium battery compounds. *J. Power Sources* **2002**, *112*, 247–254.
112. Bernardes, A.; Espinosa, D.C. R.; Tenório, J.S. Recycling of batteries: A review of current processes and technologies. *J. Power Sources* **2004**, *130*, 291–298.
113. Espinosa, D.C. R.; Bernardes, A.M.; Tenório, J.A. S. An overview on the current processes for the recycling of batteries. *J. Power Sources* **2004**, *135*, 311–319.
114. Xu, J.; Thomas, H.; Francis, R.W.; Lum, K.R.; Wang, J.; Liang, B. A review of processes and technologies for the recycling of lithium-ion secondary batteries. *J. Power Sources* **2008**, *177*, 512–527.
115. Sloop, S.E. System and Method for Removing an Electrolyte from an Energy Storage and/or Conversion Device Using a Supercritical Fluid. U.S. Patent 7198865 B2, 3 April 2007.
116. Cheret, D.; Santen, S. Battery Recycling. U.S. Patent 20050235775 A1, 27 October 2005.
117. Hanisch, C.; Haselrieder, W.; Kwade, A. Recycling von Lithium-Ionen-Batterien—Das Projekt LithoRec. In *Recycling und Rohstoffe*; Thomé-Kozmiensky, K.J., Ed.; VIVIS: Neuruppin, Germany, 2012; Volume 5, pp. 691–698.
118. Bahgat, M.; Farghaly, F.; Basir, S.A.; Fouad, O. Synthesis, characterization and magnetic properties of microcrystalline lithium cobalt ferrite from spent lithium-ion batteries. *J. Mater. Process. Technol.* **2007**, *183*, 117–121.
119. Kathryn, C.S. Solvent Extraction and Liquid Membranes. In *Solvent Extraction and Liquid Membranes*; Aguilar, M., Cortina, J.L., Ed.; CRC Press: Boca Raton, FL, USA, 2008; pp. 141–200.
120. Sun, L.; Qiu, K. Organic oxalate as leachant and precipitant for the recovery of valuable metals from spent lithium-ion batteries. *Waste Manag.* **2012**, *32*, 1575–1582.
121. Li, L.; Lu, J.; Ren, Y.; Zhang, X.X.; Chen, R.J.; Wu, F.; Amine, K. Ascorbic-acid-assisted recovery of cobalt and lithium from spent Li-ion batteries. *J. Power Sources* **2012**, *218*, 21–27.
122. Li, L.; Ge, J.; Wu, F.; Chen, R.; Chen, S.; Wu, B. Recovery of cobalt and lithium from spent lithium ion batteries using organic citric acid as leachant. *J. Hazard. Mater.* **2010,** *176*, 288–293.
123. Shin, S.M.; Kim, N.H.; Sohn, J.S.; Yang, D.H.; Kim, Y.H. Development of a metal recovery process from Li-ion battery wastes. *Hydrometallurgy* **2005**, *79*, 172–181.
124. Ferreira, D.A.; Prados, L.M. Z.; Majuste, D.; Mansur, M.B. Hydrometallurgical separation of aluminium, cobalt, copper and lithium from spent Li-ion batteries. *J. Power Sources* **2009,** *187*, 238–246.
125. Dorella, G.; Mansur, M.B. A study of the separation of cobalt from spent Li-ion battery residues. *J. Power Sources* **2007**, *170*, 210–215.
126. Zeng, G.; Deng, X.; Luo, S.; Luo, X.; Zou, J. A copper-catalyzed bioleaching process for enhancement of cobalt dissolution from spent lithium-ion batteries. *J. Hazard. Mater.* **2012**, *199*, 164–169.
127. Rothermel, S.; Evertz, M.; Kasnatscheew, J.; Qi, X.; Grützke, M.; Winter, M.; Nowak, S. Graphite Recycling from Spent Lithium-Ion Batteries. *ChemSusChem* **2016**, *9*, 3473–3484.
128. Krüger, S.; Hanisch, C.; Kwade, A.; Winter, M.; Nowak, S. Effect of impurities caused by a recycling process on the electrochemical performance of $Li[Ni_{0.33}Co_{0.33}Mn_{0.33}]O_2$. *J. Electroanal. Chem.* **2014**, *726*, 91–96.
129. Hansen, J.; Sato, M.; Kharecha, P.; Beerling, D.; Berner, R.; Masson-Delmotte, V.; Pagani, M.; Raymo, M.; Royer, D.L.; Zachos, J.C. Target atmospheric CO_2: Where should humanity aim? *arXiv preprint* **2008**, arXiv:0804.1126.
130. Donázar, J.A.; Cortés-Avizanda, A.; Fargallo, J.A.; Margalida, A.; Moleón, M.; Morales-Reyes, Z.; Moreno-Opo, R.; Pérez-García, J.M.; Sánchez-Zapata, J.A.; Zuberogoitia, I. Roles of raptors in a changing world: From flagships to providers of key ecosystem services. *Ardeola* **2016**, *63*, 181–234.
131. Pan, S.; Tian, H.; Dangal, S.R.; Yang, Q.; Yang, J.; Lu, C.; Tao, B.; Ren, W.; Ouyang, Z. Responses of global terrestrial evapotranspiration to climate change and increasing atmospheric CO_2 in the 21st century. *Earth's Future* **2015**, *3*, 15–35.
132. Rahman, S.M.; Kirkman, G.A. Costs of certified emission reductions under the Clean Development Mechanism of the Kyoto Protocol. *Energy Econ.* **2015**, *47*, 129–141.
133. Xia, W.; Vagin, S.I.; Rieger, B. Regarding initial ring opening of propylene oxide in its copolymerization with CO2 catalyzed by a cobalt (III) porphyrin complex. *Chem. Eur. J.* **2014**, *20*, 15499–15504.
134. Altenbuchner, P.T.; Kissling, S.; Rieger, B. Carbon dioxide as C-1 block for the synthesis of polycarbonates. In *Transformation and Utilization of Carbon Dioxide*; Springer: Berlin, Germany, 2014; pp. 163–200.
135. Liu, Q.; Wu, L.; Jackstell, R.; Beller, M. Using carbon dioxide as a building block in organic synthesis. *Nat. Commun.* **2015,** *6*, 5933.

136. Fang, S.; Fujimoto, K. Direct synthesis of dimethyl carbonate from carbon dioxide and methanol catalyzed by base. *Appl. Catal. A* **1996,** *142*, L1–L3.
137. Isaacs, N.S.; O'Sullivan, B.; Verhaelen, C. High pressure routes to dimethyl carbonate from supercritical carbon dioxide. *Tetrahedron* **1999**, *55*, 11949–11956.
138. Sakakura, T.; Choi, J.-C.; Saito, Y.; Sako, T. Synthesis of dimethyl carbonate from carbon dioxide: Catalysis and mechanism. *Polyhedron* **2000**, *19*, 573–576.
139. Camy, S.; Pic, J.-S.; Badens, E.; Condoret, J.-S. Fluid phase equilibria of the reacting mixture in the dimethyl carbonate synthesis from supercritical CO_2. *J. Supercrit. Fluids* **2003**, *25*, 19–32.
140. Besenhard, J.; Wagner, M.; Winter, M.; Jannakoudakis, A.; Jannakoudakis, P.; Theodoridou, E. Inorganic film-forming electrolyte additives improving the cycling behaviour of metallic lithium electrodes and the self-discharge of carbon—Lithium electrodes. *J. Power Sources* **1993**, *44*, 413–420.
141. Buqa, H.; Blyth, R.; Golob, P.; Evers, B.; Schneider, I.; Alvarez, M.S.; Hofer, F.; Netzer, F.; Ramsey, M.; Winter, M. Negative electrodes in rechargeable lithium ion batteries—Influence of graphite surface modification on the formation of the solid electrolyte interphase. *Ionics* **2000**, *6*, 172–179.
142. Buqa, H.; Golob, P.; Winter, M.; Besenhard, J. Modified carbons for improved anodes in lithium ion cells. *J. Power Sources* **2001**, *97*, 122–125.
143. Winter, M.; Imhof, R.; Joho, F.; Novak, P. FTIR and DEMS investigations on the electroreduction of chloroethylene carbonate-based electrolyte solutions for lithium-ion cells. *J. Power Sources* **1999**, *81*, 818–823.
144. Winter, M.; Novák, P. Chloroethylene Carbonate, a Solvent for Lithium-Ion Cells, Evolving CO_2 during Reduction. *J. Electrochem. Soc.* **1998,** 145, L27-L30.
145. Lide, D.; Haynes, W. *CRC Handbook of Chemistry and Physics: A Ready-Reference Book of Chemical and Physical Data/editor-in-chief, David R. Lide; associate editor, WM" Mickey" Haunes*, 90th ed.; CRC: Boca Raton, FL, USA, 2009.
146. Atkins, P.W.; De Paula, J.; Ralf, L.; Appelhagen, A. *Kurzlehrbuch Physikalische Chemie*; Wiley-VCH: Weinheim, Germany, 2008; Volume 3.
147. Henry, M.C.; Yonker, C.R. Supercritical fluid chromatography, pressurized liquid extraction, and supercritical fluid extraction. *Anal. Chem.* **2006**, *78*, 3909–3916.
148. Lack, E.; Seidlitz, H. Commercial scale decaffeination of coffee and tea using supercritical CO_2. In *Extraction of Natural Products Using Near-Critical Solvents*; Springer: Berlin, Germany, 1993; pp. 101–139.
149. Beckman, E.J. *Peer Reviewed: Using CO_2 to Produce Chemical Producs Sustainably*; ACS Publications: Washington, DC, USA, 2002.
150. Sinha, N.K.; Guyer, D.E.; Gage, D.A.; Lira, C.T. Supercritical carbon dioxide extraction of onion flavors and their analysis by gas chromatography-mass spectrometry. *J. Agric. Food Chem.* **1992**, *40*, 842–845.
151. Friedrich, J.; List, G.; Heakin, A. Petroleum-free extraction of oil from soybeans with supercritical CO_2. *J. Am. Oil Chem. Soc.* **1982**, *59*, 288–292.
152. Reverchon, E.; Senatore, F. Supercritical carbon dioxide extraction of chamomile essential oil and its analysis by gas chromatography-mass spectrometry. *J. Agric. Food Chem.* **1994**, *42*, 154–158.
153. Moisan, S.; Martinez, V.; Weisbecker, P.; Cansell, F.; Mecking, S.; Aymonier, C. General Approach for the Synthesis of Organic—Inorganic Hybrid Nanoparticles Mediated by Supercritical CO_2. *J. Am. Chem. Soc.* **2007**, *129*, 10602–10606.
154. Guironnet, D.; Gottker-Schnetmann, I.; Mecking, S. Catalytic polymerization in dense CO_2 to controlled microstructure polyethylenes. *Macromolecules* **2009**, *42*, 8157–8164.
155. Le, D.; Passerini, S.; Guo, J.; Ressler, J.; Owens, B.; Smyrl, W. High surface area V_2O_5 aerogel intercalation electrodes. *J. Electrochem. Soc.* **1996**, *143*, 2099–2104.
156. Van Bommel, M.; De Haan, A. Drying of silica aerogel with supercritical carbon dioxide. *J. Non-Cryst. Solids* **1995**, *186*, 78–82.
157. Pierre, A.C.; Pajonk, G.M. Chemistry of aerogels and their applications. *Chem. Rev.* **2002**, *102*, 4243–4266.
158. Marini, L. *Geological Sequestration of Carbon Dioxide: Thermodynamics, Kinetics, and Reaction Path Modeling*; Elsevier: Amsterdam, the Netherlands, 2006; Volume 11.
159. Span, R.; Wagner, W. A new equation of state for carbon dioxide covering the fluid region from the triple-point temperature to 1100 K at pressures up to 800 MPa. *J. Phys. Chem. Ref. Data* **1996,** *25*, 1509–1596.
160. Roth, M. Helium head pressure carbon dioxide in supercritical fluid extraction and chromatography: Thermodynamic analysis of the effects of helium. *Anal. Chem.* **1998**, *70*, 2104–2109.

161. Chiu, K.-H.; Yak, H.-K.; Wai, C.M.; Lang, Q. Dry ice-originated supercritical and liquid carbon dioxide extraction of organic pollutants from environmental samples. *Talanta* **2005**, *65*, 149–154.
162. Liu, Y.; Mu, D.; Zheng, R.; Dai, C. Supercritical CO_2 extraction of organic carbonate-based electrolytes of lithium-ion batteries. *RSC Adv.* **2014**, *4*, 54525–54531.
163. Grützke, M.; Mönnighoff, X.; Horsthemke, F.; Kraft, V.; Winter, M.; Nowak, S. Extraction of lithium-ion battery electrolytes with liquid and supercritical carbon dioxide and additional solvents. *RSC Adv.* **2015**, *5*, 43209–43217.
164. Liu, Y.; Mu, D.; Dai, Y.; Ma, Q.; Zheng, R.; Dai, C. Analysis on Extraction Behaviour of Lithium-ion Battery Electrolyte Solvents in Supercritical CO_2 by Gas Chromatography. *Int. J. Electrochem. Sci.* **2016**, *11*, 7594–7604.
165. Friesen, A.; Mönnighoff, X.; Börner, M.; Haetge, J.; Schappacher, F.M.; Winter, M. Influence of temperature on the aging behavior of 18650-type lithium ion cells: A comprehensive approach combining electrochemical characterization and post-mortem analysis. *J. Power Sources* **2017**, *342*, 88–97.
166. Kasnatscheew, J.; Schmitz, R.W.; Wagner, R.; Winter, M.; Schmitz, R. Fluoroethylene carbonate as an additive for γ-butyrolactone based electrolytes. *J. Electrochem. Soc.* **2013**, *160*, A1369–A1374.
167. Kim, G.-Y.; Petibon, R.; Dahn, J. Effects of succinonitrile (SN) as an electrolyte additive on the impedance of $LiCoO_2$/graphite pouch cells during cycling. *J. Electrochem. Soc.* **2014**, *161*, A506–A512.
168. Leggesse, E.G.; Jiang, J.-C. Theoretical study of the reductive decomposition of 1,3-propane sultone: SEI forming additive in lithium-ion batteries. *RSC Adv.* **2012**, *2*, 5439–5446.